MOLECULAR AND CELLULAR BIOLOGY, Oct. 2008, p. 6248–6261 Vol. 28, No. 20
0270-7306/08/$08.00+0 doi:10.1128/MCB.00795-08

Lactate Stimulates Vasculogenic Stem Cells via the Thioredoxin System and Engages an Autocrine Activation Loop Involving Hypoxia-Inducible Factor 1[▽]

Tatyana N. Milovanova,[1] Veena M. Bhopale,[1] Elena M. Sorokina,[1] Jonni S. Moore,[2] Thomas K. Hunt,[3] Martin Hauer-Jensen,[4] Omaida C. Velazquez,[5] and Stephen R. Thom[1,6]*

Institute for Environmental Medicine[1] and Departments of Pathology and Laboratory Medicine[2] and Emergency Medicine,[6] University of Pennsylvania Medical Center, Philadelphia, Pennsylvania 19104; Department of Surgery, University of California at San Francisco, San Francisco, California 14143[3]; Department of Surgery, University of Arkansas for Medical Sciences, Little Rock, Arkansas[4]; and Department of Surgery, University of Miami, Miami, Florida[5]

Received 16 May 2008/Returned for modification 19 June 2008/Accepted 1 August 2008

The recruitment and differentiation of circulating stem/progenitor cells (SPCs) in subcutaneous Matrigel in mice was assessed. There were over one million CD34$^+$ SPCs per Matrigel plug 18 h after Matrigel implantation, and including a polymer to elevate the lactate concentration increased the number of SPCs by 3.6-fold. Intricate CD34$^+$ cell-lined channels were linked to the systemic circulation, and lactate accelerated cell differentiation as evaluated based on surface marker expression and cell cycle entry. CD34$^+$ SPCs from lactate-supplemented Matrigel exhibited significantly higher concentrations of thioredoxin 1 (Trx1) and hypoxia-inducible factor 1 (HIF-1) than cells from unsupplemented Matrigel, whereas Trx1 and HIF-1 in CD45$^+$ leukocytes were not elevated by lactate. Results obtained using small inhibitory RNA (siRNA) specific to HIF-1 and mice with conditionally HIF-1 null myeloid cells indicated that SPC recruitment and lactate-mediated effects were dependent on HIF-1. Cells from lactate-supplemented Matrigel had higher concentrations of phosphorylated extracellular signal-regulated kinases 1 and 2, Trx1, Trx reductase (TrxR), vascular endothelial growth factor (VEGF), and stromal cell-derived factor 1 (SDF-1) than cells from unsupplemented Matrigel. SPC recruitment and protein changes were inhibited by siRNA specific to lactate dehydrogenase, TrxR, or HIF-1 and by oxamate, apocynin, U0126, *N*-acetylcysteine, dithioerythritol, and antibodies to VEGF or SDF-1. Oxidative stress from lactate metabolism by SPCs accelerated further SPC recruitment and differentiation through Trx1-mediated elevations in HIF-1 levels and the subsequent synthesis of HIF-1-dependent growth factors.

Neovascularization plays a central role in wound healing and tumor growth. In both wounds and tumors, the local tissue lactate concentration is elevated and reaches ~6 to 15 mM, in contrast to a concentration of 1.8 to 2 mM under normal physiological conditions (14, 53). Lactate has been reported to be proangiogenic, and substantial attention has been focused on endothelial cell responses in wounds and tumors (10, 13). Whether lactate plays a direct role in vasculogenesis, that is, homing and vascular channel formation by stem/progenitor cells (SPCs), however, is unknown.

We hypothesized that lactate augments SPC growth and differentiation by stimulating an oxidative stress response. There is a growing body of evidence demonstrating that reactive oxygen species (ROS) exert roles in transduction cascades of growth factors which regulate cell proliferation and differentiation (38). Local elevations in lactate can increase cellular NADH levels through the action of lactate dehydrogenase (LDH), and this effect will secondarily increase intracellular ROS production by stimulating NAD(P)H oxidase (Nox) enzymes (19, 31). Lactate can also enhance free-radical formation via Fenton-like reactions (1, 19).

Thioredoxin (Trx) is a ubiquitous disulfide oxidoreductase that works in conjunction with the glutathione system to maintain the cytoplasm in a reduced state. The Trx system includes the Trx1 cytosolic and Trx2 mitochondrial thiol proteins, Trx reductase (TrxR), and NADPH. Oxidative stress increases Trx1 synthesis and the translocation of Trx1 to the nucleus, where it acts as a growth factor and transcription factor regulator (3, 12, 21, 36, 40). There are redundant systems for maintaining Trx1 in a reduced state, which is fundamental to regulating its functions. Knocking down TrxR by either enzyme inhibitors or small inhibitory RNA (siRNA) significantly depletes the cellular concentration of reduced Trx1 under conditions of oxidative stress (54).

Trx1 has been shown previously to promote the expression and activity of hypoxia-inducible factor 1 (HIF-1) (12, 26, 55). HIF-1 is a heterodimer composed of HIF-1α and constitutively expressed HIF-β (also called the aryl hydrocarbon receptor nuclear translocator subunit). The expression and activation of the HIF-1α subunit are tightly regulated, and HIF-1α degradation by the ubiquitin-proteasome pathway typically occurs when cells are replete with O_2 (42, 44). Recent gene array data suggest that lactate can upregulate HIF-1 in mesenchymal stem cells, but its functional significance, as well as proximal factors that mediate this response, is unclear (60). Trx1 can

* Corresponding author. Mailing address: Institute for Environmental Medicine, University of Pennsylvania, 1 John Morgan Building, 3620 Hamilton Walk, Philadelphia, PA 19104-6068. Phone: (215) 898-9095. Fax: (215) 573-7037. E-mail: sthom@mail.med.upenn.edu.

▽ Published ahead of print on 18 August 2008.

increase HIF-1 protein expression under both normoxic and hypoxic conditions (55), leading us to hypothesize that HIF-1 may be an important factor in SPC biology.

HIF-1 coordinates cell responses important for neovascularization, including the synthesis of vascular endothelial growth factor (VEGF) and stromal cell-derived factor 1 (SDF-1) (44). These growth factors, and others, are synthesized by local endothelial cells, perivascular myofibroblasts, keratinocytes, macrophages, bone marrow-derived hemangiocytes, and endothelial progenitor cells (EPCs) recruited to the wound site (18, 25, 33, 43, 45). Growth factors influence the efficiency of new blood vessel growth by angiogenesis involving local endothelial cells, and they stimulate the recruitment and differentiation of circulating SPCs to form vessels by vasculogenesis (15, 22, 39, 46, 50, 58). Endothelial cells respond to lactate by increasing the synthesis of VEGF in a process that may involve the stabilization of HIF-1 (23). Lactate and pyruvate are interconvertible via the enzymatic action of LDH. Both can stabilize HIF-1 by oxidizing cellular iron, which inhibits prolyl hydroxylase activity that requires ferrous iron (10, 13, 32).

We hypothesized that SPCs metabolize lactate and thereby play an active role in their own recruitment and differentiation at sites peripheral to the bone marrow. Results showed that SPCs were among the earliest cells to arrive at a subcutaneous Matrigel target. In the presence of high lactate concentrations, SPCs synthesized markedly higher amounts of Trx1, TrxR, and HIF-1, as well as VEGF and SDF-1, than in the absence of such concentrations. $CD45^+$ leukocytes were also recruited to Matrigel, but in much lower numbers than the SPCs, and the $CD45^+$ cells did not express elevated Trx1 and HIF-1 in the presence of lactate. To more discretely evaluate the role of HIF-1, we utilized siRNA specific to HIF-1 and also genetically modified mice in which Cre recombinase synthesis was linked to the lysozyme gene and *loxP* flanked the HIF-1 gene locus. This approach causes conditionally HIF-1 null myeloid cells (9). Because a subpopulation of bone marrow SPCs intermittently express lysozyme, we reasoned that these mice would be useful in investigating HIF-1-deficient SPCs (57). Results with these mice and with siRNA targeting HIF-1 showed that SPC homing was mediated through HIF-1. Cells recruited to Matrigel in these mice synthesized significantly less Trx1, TrxR, VEGF, and SDF-1 and exhibited lower fractions of phosphorylated mitogen-activated protein kinases (MAPKs) than cells recruited in wild-type mice, and $CD34^+$ SPC recruitment to Matrigel in these mice was diminished compared to that in wild-type mice. These in vivo observations indicate that an autocrine activation loop exists in SPCs whereby growth factors mediate the phosphorylation of MAPKs that cause the elevation of transcription factor levels, analogous to ex vivo observations made with endothelial cells and some tumor lines (11, 48). Because HIF-1 stimulates VEGF and SDF-1 synthesis, SPCs augment their own recruitment.

MATERIALS AND METHODS

Animal study procedures. Wild-type mice (*Mus musculus*) were purchased from Jackson Laboratories (Bar Harbor, ME), given a standard rodent diet and water ad libitum, and housed in the animal facility of the University of Pennsylvania. In some studies, we used mice developed by Randall S. Johnson at the University of California, San Diego, that had conditionally HIF-1 null myeloid cells. In these mice, Cre recombinase cDNA was inserted into the endogenous myeloid lysozyme locus and *loxP* flanked the HIF-1 locus.

The standard protocol was to place two subcutaneous Matrigel plugs into each mouse, one on either side of the thoracic vertebrae. Matrigel is an endothelial cell basement membrane-like material that is a liquid at 0°C and a solid at body temperature (29). After anesthetization (intraperitoneal administration of ketamine [100 mg/kg of body weight] and xylazine [10 mg/kg]), the skin was prepared by being swabbed with Betadine, and Matrigel plugs (1 ml) were injected subcutaneously into the back on either side of the thoracic vertebrae. One of the Matrigel plugs was supplemented with DL-lactide (85 mol%; 32 mg/ml of Matrigel). This polymer is hydrolyzed slowly so that, when applied to wounds, it sustains the lactate monomer concentration within a range of ~6 to 15 mM (51). In our studies, the slow degradation of the lactate polymer resulted in a lactate concentration in Matrigel of 16.2 ± 0.4 mM (mean ± standard error [SE]; $n = 3$) at 18 h after implantation versus 3.5 ± 0.7 mM ($n = 3$; $P < 0.05$) in unsupplemented Matrigel. Levels remained stable over the course of the experiment, and at 10 days, values were 15.8 ± 0.3 mM ($n = 3$) for lactide-supplemented Matrigel and 3.8 ± 0.5 mM ($n = 3$) for unsupplemented Matrigel. Lactate concentrations in digested Matrigel were measured by the EnzyChrom lactate assay kit (Bioassay Systems, Hayward, CA). Where indicated, Matrigel was supplemented with 15 mM oxamate, 10 μM mitomycin C, 0.1 mM apocynin, 1 μM dithioerythritol (DTE), 5 μM *N*-acetylcysteine (NAC), 14 μM 1,4-diamino-2,3-dicyano-1,4,6-(2-aminophenylthio)butadiene (U0126; Calbiochem, San Diego, CA), 10 μg of anti-VEGF or anti-SDF-1 (BD Biosciences, San Diego, CA), or 37.5 ng of siRNA specific to HIF-1 or TrxR or nonsilencing control siRNA conjugated to Alexa Fluor 488 (Qiagen, Germantown, MD) or 37.5 ng of siRNA specific to mouse LDH (Santa Cruz).

At selected times, mice were reanesthetized and blood was obtained into heparinized syringes by cardiac puncture. Matrigel plugs were harvested and sharply cut with a blade, and approximately one-third of each plug was placed into MethoCult colony assay medium (StemCell Technologies, Vancouver, British Columbia) for incubation at 37°C in air with 5% CO_2 under a fully humidified atmosphere. A second, small slice of the Matrigel was placed onto a glass slide for staining with 10 μM dihydro-2′,7′-dichlorofluorescein (H_2DCF; Kodak, Rochester, NY) diacetate or fluorochrome-conjugated antibodies for microscopic examination, and the remaining Matrigel plug was weighed in a plastic dish and then digested by incubation with 1 ml of dispase for 90 min at 37°C. Bone marrow cells were also obtained from both femurs. The ends of each bone were clipped, and the marrow cavities were flushed with 2 ml of phosphate-buffered saline (PBS). Leukocytes were isolated from blood samples, samples of Matrigel digested with dispase, and bone marrow samples for cell counting, flow cytometry analysis, and Western blotting of cell lysates. In addition, the cells from digested Matrigel were frozen and subjected to Western blotting at later times. In brief, 5×10^6 cells from each sample type (Matrigel, blood, and bone marrow) were lysed, the protein concentration was adjusted to 25 mg/ml, 5 μg of protein was placed into each lane, and Western blotting was performed by following previously described methods (49). Antibodies used for Western blotting were against HIF-1 (R&D, Minneapolis, MN), mouse thioredoxin-1 (Cell Signaling Technology, Danvers, MA), and the MAPKs extracellular signal-regulated kinases 1 and 2 (ERK 1/2) and Jun N-terminal protein kinase (JNK) (Santa Cruz) and p38 (BD Pharmingen). MAPK antibodies included antibodies specific for the phosphorylated forms and antibodies recognizing both phosphorylated and nonphosphorylated forms.

Flow cytometry. Flow cytometry was performed with a 4-color, dual-laser analog FACSCalibur system (Becton Dickinson, San Jose, CA) using CellQuest acquisition software or with an 18-color LSRII system (BD Biosciences, San Diego, CA) using FACSDiva digital acquisition electronics and software (BD Biosciences) by standard protocols (5, 17, 52). Cells were gated based on forward and side laser light scattering, and nucleated cells were segregated from debris by DRAQ5 DNA staining. To identify SPCs, we utilized specific anti-mouse fluorochrome-conjugated antibodies: anti-mouse CD34-fluorescein isothiocyanate (anti-CD34-FITC) and CD34-phycoerythrin (anti-CD34-PE; eBioscience, San Diego, CA); anti-mouse Sca-1–FITC (BD Pharmingen); anti-mouse CXCR4-allophycocyanin (anti-CXCR4-APC; R&D, Minneapolis, MN); and anti-mouse VEGF receptor 2 (VEGFR2)–Flk-1–APC, von Willebrand factor (vWF)-FITC, CD133-APC, and TER119-FITC (eBioscience).

For cell cycle analysis, leukocytes (10^6) were pelleted and fixed with 70% ice-cold ethanol and then incubated with RNase (100 μg/ml) and propidium iodide (4 μg/ml) in PBS or Vindelov's reagent containing Tris (pH 7.6), 1 mg of RNase A, 7.5 mg of propidium iodide, and 0.1 ml of Nonidet P-40, stored at 4°C, and labeled at room temperature (RT). SPCs labeled with anti-CD34-FITC were permeabilized with 2% paraformaldehyde for 20 min on ice, followed by 0.1% Triton X-100 for 5 min at RT. Flow cytometry was performed by collecting 6 ×

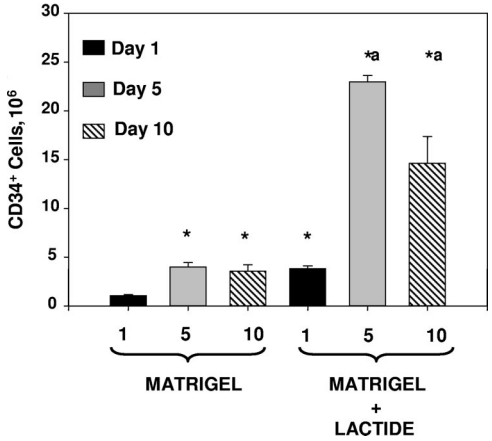

FIG. 1. Counts of $CD34^+$ cells in Matrigel plugs. Plugs were digested with dispase, stained with fluorochrome-tagged antibodies, and suspended in PBS. The total number of cells in each sample was calculated based on the volume of the cell suspension and the rate at which fluid was taken up in the flow cytometer. *, significantly different from cell number in unsupplemented Matrigel harvested at 18 h (day 1); *a*, significantly different from cell numbers in unsupplemented Matrigel samples harvested at 5 and 10 days. Cell counts in Matrigel-lactide at 5 versus 10 days postimplantation were also significantly different. Numbers are means ± SE ($n = 5$) for all groups.

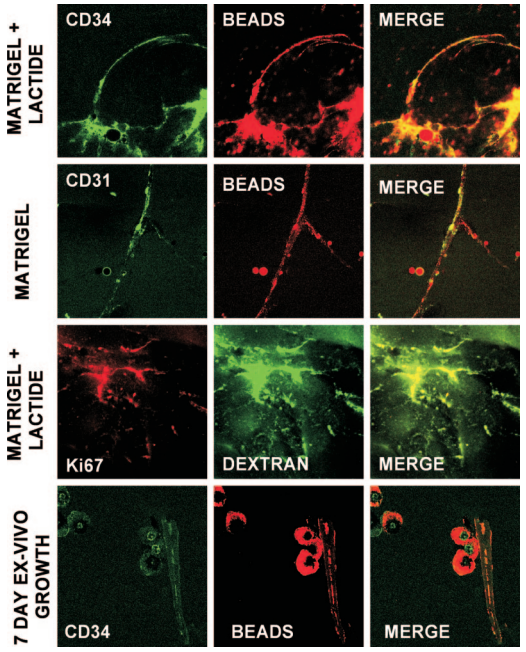

FIG. 2. SPC surface marker expression and vascular channels identified by dextran and Nile red beads in Matrigel harvested 18 h postimplantation. Note that each row shows images from different samples. The bottom row shows images of Matrigel harvested at 18 h and incubated ex vivo for 7 days.

10^4 events gating solely on $CD34^+$ cells, and the percentage of cells in each cycle phase was analyzed by using ModFit *LT* cell cycle analysis software (Verity Software House).

Trx and HIF-1 staining for flow cytometry. Isolated leukocytes (5×10^5) were pelleted and fixed with 4% paraformaldehyde at RT for 20 min and then washed twice with PBS. Cells were resuspended in 200 μl of SAP buffer (2% fetal bovine serum, 0.5% saponin, and 0.1% sodium azide in PBS), and anti-mouse Trx1 or anti-HIF-1α antibody was added at the final concentration of 10 μg/ml. Samples were incubated for 20 min at RT and then washed twice with SAP buffer. Cells were resuspended in 200 μl of SAP buffer and stained with 5 μl of secondary goat anti-mouse APC-conjugated immunoglobulin G (eBioscience). Following incubation for 20 min at RT, cells were washed once with SAP buffer and once with PBS and resuspended in 250 μl of PBS. Conjugated antibodies—2 μl of anti-β-actin–FITC (Sigma), 2 μl of anti-CD34-PE (eBioscience), 1 μl of anti-DRAQ5 (Alexis), and 2 μl of antistreptavidin-APC (eBioscience)—were added for 1 h on ice, and cells were washed twice in PBS before four-color fluorescence-activated cell sorter analysis. Anti-β-actin was measured in the FL1 channel (530/30-nm band-pass filter), anti-CD34–*R*-PE was measured in the FL2 channel (585/42-nm band-pass filter), anti-DRAQ5 (nucleic acid stain) was measured in the FL3 channel (670-nm long-pass filter) by excitation from the 488-nm blue laser, and anti-HIF-1–APC was measured in the FL4 channel (661/16-nm band-pass filter) by excitation from the 635-nm red diode laser. Compensation for HIF-1–APC in multiparameter flow cytometry is dose dependent and was determined empirically after acquiring 50,000 events per sample. Dead cells and debris were excluded based on forward-angle and side scattering. Side scatter gating on the $DRAQ5^+$ population was used to distinguish nucleated cells, and anti-β-actin–FITC confirmed the uniform permeabilization of SPCs. Data were analyzed using CellQuest (Becton Dickinson) and FlowJo (TreeStar) software. To compare the percentages of cells positive for HIF-1, all cells with *R*-PE, FITC, DRAQ5, and APC fluorescence intensities above 98% of the mean intensities of the control samples were considered. The controls were developed from samples in which one specific antibody had been omitted, and four-color compensation was empirically assessed.

Confocal microscopy. Confocal microscopy with a Radiance 2000 system (Bio-Rad, Hercules, CA) was used to create images of vascular channels and cells recruited into Matrigel. Matrigel implants were thinly sliced, and cells were labeled with specific anti-mouse CD34-FITC, TER119-FITC, vWF-FITC, or CD31-FITC in 1:100 dilutions for 60 min on ice and then placed onto a glass slide for observation at magnifications of ×600 and five times greater. The presence of functional vascular channels in the Matrigel was documented by injecting mice with carboxylate-modified polystyrene beads (FluoSpheres [0.04 μm; Invitrogen]) conjugated to Nile red or with FITC-conjugated dextran (molecular weight, 40,000; Invitrogen, Inc.) by procedures described by Springer et al. (47). To quantify the fluorescence of DCF in $CD34^+$ cells, the relative fluorescence intensities of samples with and without the addition of 24 mM KCl to cause cell depolarization were measured.

Statistical analysis. Results are expressed as the means ± SE of values obtained in three or more independent experiments. To compare data, we used a one-way analysis of variance with SigmaStat (Jandel Scientific, San Jose, CA) and the Newman-Keuls post hoc test or Student's *t* test where appropriate. The level of statistical significance was defined as a P value of <0.05.

RESULTS

Cell recruitment to Matrigel. Plugs were harvested 18 h (day 1) or 5 or 10 days after implantation and digested so that cells in the Matrigel could be characterized by flow cytometry. At 18 h postimplantation, 97.5% ± 0.3% of all cells in Matrigel expressed the SPC marker CD34, and 93.7% ± 0.6% (not significant [NS]; $n = 5$ samples in each group) of cells in Matrigel-lactide were $CD34^+$. As shown in Fig. 1, there was a consistent pattern, with increasing numbers of $CD34^+$ cells in Matrigel versus Matrigel-lactide from 18 h to 5 days but no significant increase in samples harvested 10 days after implantation.

Vascular channels in Matrigel. To assess whether vascular channels developed in the Matrigel, anesthetized mice underwent intracardiac infusion with fluorescein-conjugated dextran or Nile red beads prior to the harvesting of Matrigel (Fig. 2). Even at just 18 h after implantation, channels could be visualized. $CD34^+$ cells lined these channels, and many of the channels also expressed the EPC marker CD31 and the mitotic marker Ki67. There appeared to be a greater number of channels, with more interconnections, in Matrigel supplemented with the lactate polymer than in unsupplemented Matrigel.

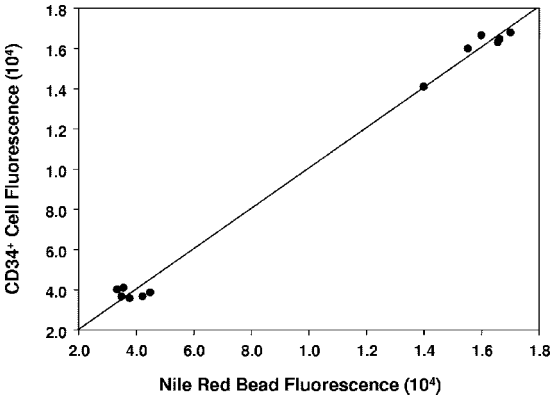

FIG. 3. The relationship between Nile red bead fluorescence in Matrigel plugs and fluorescence from $CD34^+$ cells is shown. Matrigel was stained with FITC-conjugated anti-CD34 antibody, and fluorescence in green and red channels was quantified as outlined in Materials and Methods. The six data points closest to the origin are for unsupplemented Matrigel, whereas the six in the upper right corner are for Matrigel with lactide. Values are relative fluorescence units.

The pattern was complex, however, and not amenable to simply counting channels. Therefore, we quantified the fluorescence of $CD34^+$ cells as well as fluorescence from Nile red beads. There was a linear correlation between cell fluorescence and Nile red bead fluorescence (Fig. 3). The intensities of cell and Nile red bead fluorescence in unsupplemented Matrigel were, respectively, $3.8 \times 10^4 \pm 1.8 \times 10^4$ relative fluorescence units (mean ± SE; $n = 6$) and $3.8 \times 10^4 \pm 0.9 \times 10^4$ relative fluorescence units ($n = 6$), versus those in Matrigel-lactide of $1.6 \times 10^5 \pm 0.4 \times 10^5$ relative fluorescence units ($n = 6$; $P < 0.05$) and $1.6 \times 10^5 \pm 0.4 \times 10^5$ relative fluorescence units ($n = 6$; $P < 0.05$). If the harvested Matrigel was cultured ex vivo for 7 days, the linear structures present at the time of removal could be detected based on the presence of intravascular fluorescent markers, and there were also many unorganized clumps of $CD34^+$ cells (Fig. 2).

Cell recruitment versus proliferation. Matrigel plugs with or without lactide that contained 15 μM mitomycin C were harvested 18 h after implantation, and essentially the same numbers of $CD34^+$ cells as those in control Matrigel samples were found (Table 1). The cytostatic impact of mitomycin C was apparent, however, based on an assessment of annexin V expression to evaluate cell apoptosis. There were only 5.9% ± 1.8% (mean ± SE; $n = 5$) apoptotic $CD34^+$ cells in unsupplemented Matrigel control samples harvested 18 h after implantation, whereas samples containing mitomycin C had 62.3% ± 2.3% ($n = 3$; $P < 0.05$) apoptotic cells. Lactide-supplemented Matrigel had 4.6% ± 0.8% (mean ± SE; $n = 5$) apoptotic $CD34^+$ cells, and lactide-supplemented samples containing mitomycin C had 66.0% ± 3.1% ($n = 3$; $P < 0.05$) apoptotic cells.

To explore further the contribution of cell proliferation to increasing cell numbers, Matrigel plugs were also harvested from mice 5 days after implantation or 18 h after implantation and incubated ex vivo for 7 days. As expected, these samples exhibited marked increases in SPC numbers versus cell counts at 18 h, although cells incubated ex vivo appeared to form clumps instead of linear networks (Table 2; Fig. 2). Lactide-containing Matrigel had more cells than unsupplemented Matrigel.

SPC characterization. Surface markers in addition to CD34 were evaluated to assess cell lineage more precisely. A typical flow cytometry analysis of cells from Matrigel and Matrigel-lactide is shown in Fig. 4. Table 3 reports the coexpression of markers on $CD34^+$ cells from samples of bone marrow, blood, and Matrigel with or without lactide harvested 18 h after implantation. The fractions of cells exhibiting putative SPC markers, including dim surface expression of CD45 ($CD45^-$) and the expression of Sca-1, CD133, and CXCR4, in blood samples were lower than those in bone marrow samples, as expected (4). The proportions of $CD34^+$ cells that coexpressed dim CD45, Sca-1, CD133, and CXCR4 in Matrigel samples (with or without lactide) were significantly higher than those in blood samples. EPCs are thought to express CD31 and VEGFR2. The levels of CD31 coexpression on $CD34^+$ cells in Matrigel samples were significantly higher than those in blood samples. VEGFR2 was expressed on 97% of blood $CD34^+$ cells, and so no difference compared to cells in Matrigel was noted. Very small fractions of $CD34^+$ cells in blood and unsupplemented Matrigel samples expressed vWF, but there was a significant increase in such cells in Matrigel supplemented with lactide. We also evaluated the expression of TER119, a surface marker for cells following an erythroid lineage (28), because we observed erythrocytes in the Matrigel vascular channels. Whereas very few $CD34^+$ cells in the blood samples expressed TER119, the proportion was elevated among cells harvested from Matrigel plugs.

If Matrigel was harvested at 5 days postimplantation, versus at 1 day, there were more $CD34^+$ cells in lactide-supplemented samples than in Matrigel-only samples and nearly one-quarter of $CD34^+$ cells in Matrigel with or without lactide coexpressed

TABLE 1. $CD34^+$ cell counts (10^6) in Matrigel samples[a]

Mouse background	Inhibitor (no. of samples evaluated)	$CD34^+$ cell count (10^6) in:	
		Matrigel	Matrigel-lactide
Wild type	None (control; 5)	1.37 ± 0.08	4.21 ± 0.18*
	Mitomycin C (3)	1.70 ± 0.06	4.80 ± 0.11*
	Control siRNA (3)	1.26 ± 0.12	3.82 ± 0.18*
	siRNA targeting LDH (3)	0.87 ± 0.03	1.70 ± 0.11*
	Oxamate (3)	0.41 ± 0.07	1.18 ± 0.43*
	Anti-VEGF (3)	0.55 ± 0.04	2.08 ± 0.03*
	Anti-SDF1 (3)	0.24 ± 0.04	0.58 ± 0.02*
	Apocynin (3)	0.66 ± 0.06	1.35 ± 0.03*
	NAC (3)	0.82 ± 0.06	1.67 ± 0.09*
	DTE (3)	0.80 ± 0.02	1.51 ± 0.09*
	U0126 (3)	1.03 ± 0.09	1.75 ± 0.10*
HIF-1 null	None (3)	0.88 ± 0.05	1.60 ± 0.12*
Control for HIF-1 null mice	None (3)	1.39 ± 0.05	4.04 ± 0.17

[a] Numbers are means ± SE. *, significantly different from value for unsupplemented Matrigel. The inclusion of any of the agents listed, except mitomycin C and nonsilencing control siRNA, resulted in cell counts significantly different from those in the corresponding control samples (Matrigel or Matrigel-lactide samples) without the inhibitor. The lower two rows show data for mice with conditionally HIF-1 null myeloid cells or control mice that were otherwise genetically identical to the conditionally null mice.

TABLE 2. $CD34^+$ cell counts and proportions of $CD34^+$ cells coexpressing CD45 or TER119 in Matrigel samples[a]

Sample group	$CD34^+$ cell count (10^6) in:		% of $CD34^+$ cells coexpressing CD45 in:		% of $CD34^+$ cells coexpressing TER119 in:	
	Matrigel	Matrigel-lactide	Matrigel	Matrigel-lactide	Matrigel	Matrigel-lactide
Samples harvested 18 h postimplantation ($n = 5$)	1.37 ± 0.08	4.21 ± 0.18*	5.2 ± 0.12	12.2 ± 0.12*	42.2 ± 1.1	46.3 ± 0.88
Samples harvested 5 days postimplantation ($n = 5$)	4.05 ± 0.45†	22.91 ± 0.67*†	22.1 ± 3.1†	25.9 ± 0.9†	24.5 ± 1.6†	68.6 ± 2.1*†
Samples harvested 18 h postimplantation and incubated ex vivo for 7 days ($n = 5$)	31.5 ± 6.1†	88.3 ± 2.03*†	44.1 ± 1.1†	81.3 ± 6.2*†	39.5 ± 1.6	48.6 ± 2.8*

[a] Numbers are means ± SE. *, significantly different from value for unsupplemented Matrigel samples; †, significantly different from value in same column for 18-h sample.

the panhematopoietic marker CD45 (Table 2). Significantly more cells in Matrigel samples containing lactide than in Matrigel-only samples coexpressed TER119. The influence of lactate on cell differentiation was also demonstrated by the examination of several surface markers on $CD34^+$ cells from Matrigel harvested 18 h after implantation and incubated ex vivo for 7 days. A significantly higher proportion of these cells than of cells from Matrigel at 18 h postimplantation expressed CD45, whereas changes in TER119 expression were variable (Table 2).

Lactate metabolism and the role of growth factors. As outlined in the introduction, we hypothesized that lactate metabolism and growth factors such as VEGF and SDF-1 influence SPC responses. Significantly fewer $CD34^+$ cells were found in Matrigel harvested at 18 h postimplantation when it contained siRNA targeting LDH or 15 mM oxamate, a competitive inhibitor of LDH (35) (Table 1). The inclusion of neutralizing antibodies against VEGF or SDF-1 within the Matrigel also inhibited increases in $CD34^+$ cells.

Reactive species and effects of antioxidants. We hypothesized that lactate metabolism causes oxidative stress mediated by Nox enzymes. Matrigel was harvested 18 h postimplantation and stained with H_2DCF, and the conversion of H_2DCF to fluorescent DCF was measured to assess ROS production (Fig. 5). Because there were different numbers of cells in the samples, the quantitative analysis of fluorescence required analyzing duplicate samples incubated with 24 mM KCl to cause cell depolarization. In this way, the relative fluorescence in each sample was quantified as the ratio of the fluorescence in the absence of KCl to that in the presence of KCl. An example of the images observed is shown in Fig. 5, along with the data analysis. The fluorescence ratio was significantly higher for Matrigel containing lactide than for unsupplemented Matrigel. If the Matrigel samples contained LDH-specific siRNA, there was no significant difference between the results for Matrigel without and Matrigel with lactide. Moreover, fluorescence ratios for Matrigel samples containing the siRNA were significantly lower than those for Matrigel samples prepared in the standard fashion.

To assess the impact of oxidative stress on $CD34^+$ cell recruitment, a number of inhibitory agents were included in Matrigel samples. The inclusion of 0.1 mM apocynin, a Nox inhibitor, or the antioxidant NAC or DTE significantly reduced the number of $CD34^+$ cells in Matrigel samples harvested 18 h after implantation (Table 1).

Trx1 and HIF-1 expression in cells recruited to Matrigel by 18 h postimplantation. By flow cytometry, cells found in Matrigel samples harvested 18 h after implantation were partitioned into $CD34^+$ SPCs and leukocytes that expressed CD45 but not CD34, and the intracellular expression of Trx1 and HIF-1 was evaluated. As shown in Table 4, the number of $CD34^-$ $CD45^+$ leukocytes was small, and such cells in Matrigel-lactide samples did not exhibit significant differences in the expression of Trx1 or HIF-1 from those in unsupplemented Matrigel samples, whereas the $CD34^+$ cells in Matrigel-lactide samples exhibited significantly greater expression of Trx1 and HIF-1 than those in unsupplemented Matrigel samples. The same patterns of protein expression were found in cell lysates analyzed by Western blotting (see Fig. 7 and 8).

Roles of Trx and HIF-1 in SPC recruitment. The recruitment of SPCs to Matrigel was evaluated with the inclusion of siRNA targeting TrxR or HIF-1 (Table 4). As expected, there was a marked reduction in the number of cells and also the HIF-1 content in the cells obtained from Matrigel containing siRNA specific to HIF-1. Because we observed elevations of Trx1 in $CD34^+$ cells isolated from lactate-supplemented Matrigel samples, we also evaluated the impact of siRNA targeting TrxR. Cell numbers were significantly reduced in these samples, and notably, there was a reduction of Trx1. Of greater surprise, we found a reduction in HIF-1 expression in these $CD34^+$ cells, suggesting a complex interaction between the Trx system and HIF-1. Contrary to those in $CD34^+$ cells, the levels of HIF-1 and Trx1 in $CD45^+$ cells from Matrigel containing TrxR-specific siRNA were not significantly decreased.

The role of HIF-1 in SPC homing to Matrigel was next evaluated in a series of studies conducted with mice with conditionally HIF-1 null myeloid-lineage cells. Based on flow cytometry results, the $CD34^+$ cell populations in blood and Matrigel-lactide samples had virtually no HIF-1 and those in bone marrow samples had only very small amounts (Fig. 6). In these studies, as well as the flow cytometry trials comparing $CD34^+$ SPCs and $CD45^+$ leukocytes, cell permeabilization was always assessed directly by measuring the fluorescence of β-actin in the cell samples. Dot plots demonstrating the uniform staining among samples are shown in Fig. 6.

Interestingly, although the leukocyte counts in blood sam-

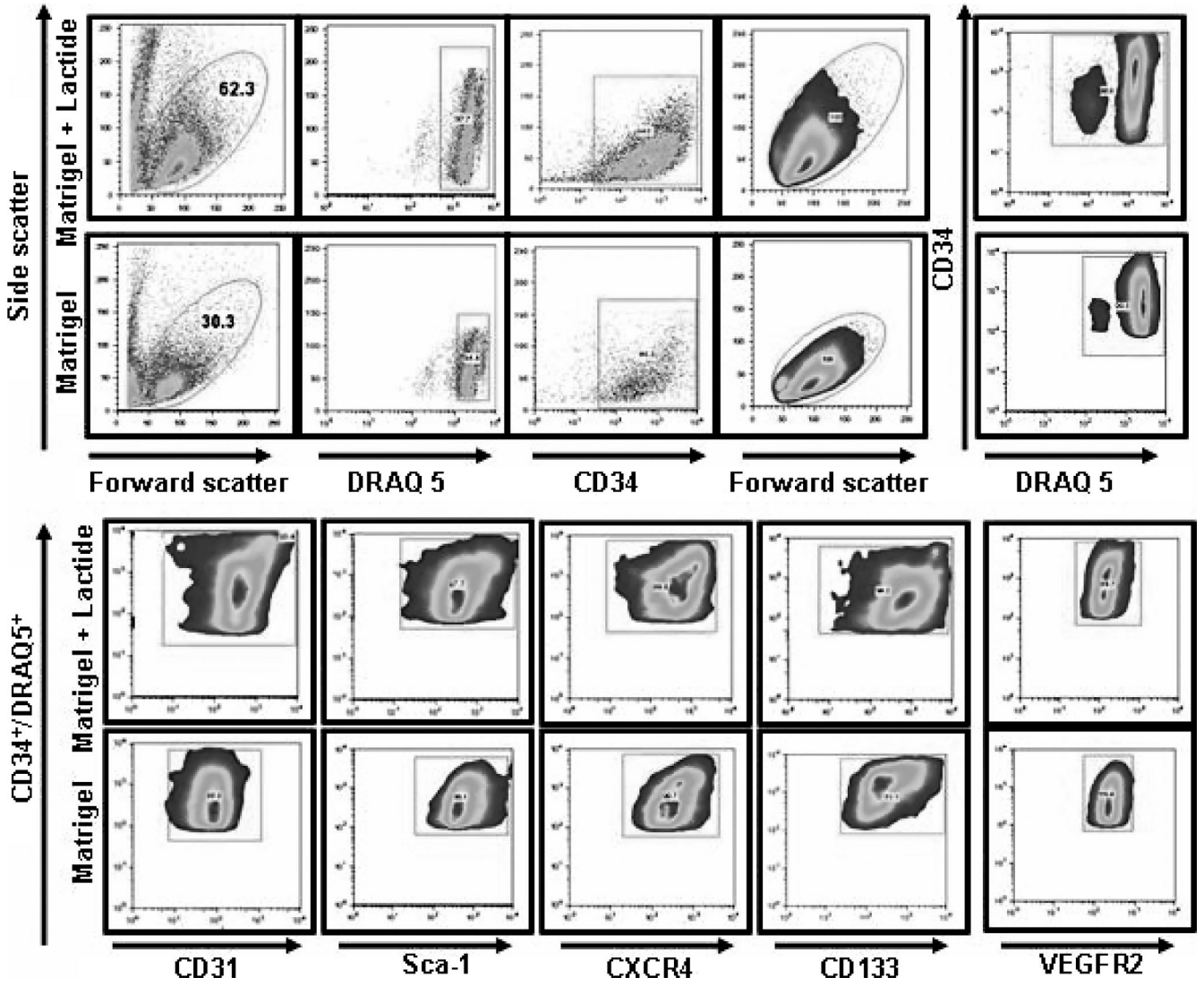

FIG. 4. SPC flow cytometry analysis protocol. Leukocytes in Matrigel with or without lactide were evaluated based on forward and side laser light scattering, and the circled populations were selected for further analysis. SPCs were enumerated based on the surface expression of CD34 and DNA staining using DRAQ5. $CD34^+$ $DRAQ5^+$ cells were then evaluated for the expression of CD31, Sca-1, CXCR4, CD133, and VEGFR2.

TABLE 3. Surface markers expressed on $CD34^+$ cells evaluated by four-color flow cytometry[a]

Surface marker	% of $CD34^+$ $DRAQ5^+$ cells expressing marker in samples of:			
	Bone marrow	Blood	Matrigel	Matrigel-lactide
Dim CD45 expression ($CD45^-$)	94 ± 3	80 ± 4*	95 ± 2	88 ± 2*
Sca-1	95 ± 2	79 ± 3*	96 ± 1	92 ± 3
CD133	90 ± 4	66 ± 2*	95 ± 3	82 ± 3*
CXCR4	78 ± 2	56 ± 5*	90 ± 5*	80 ± 5
CD31	4 ± 2	46 ± 4*	82 ± 4*	86 ± 3*†
VEGFR	6 ± 2	97 ± 2*	92 ± 4*†	90 ± 4*†
vWF	26 ± 3*	4 ± 1	6 ± 2†	66 ± 4*
TER119	42 ± 3	3 ± 1*	42 ± 4	42 ± 6

[a] A minimum of 50,000 $CD34^+$ cells were counted for each sample, and data are means ± SE ($n = 5$ samples). *, significantly different from other values in row; †, not significantly different from value to the immediate left in same row.

ples from HIF-1 null mice did not differ from those in samples from wild-type mice, the percentages of $CD34^+$ cells in blood samples from conditionally HIF-1 null mice were markedly different. Wild-type mice had 0.4% ± 0.05% ($n = 5$) $CD34^+$ cells, whereas the mice with conditionally HIF-1 null myeloid cells had 3.2% ± 0.01% ($P < 0.05$; $n = 4$) $CD34^+$ cells. The level of $CD34^+$ cell recruitment to Matrigel in conditionally HIF-1 null mice was markedly lower than that in wild-type mice (Table 1). In control mice that were otherwise genetically identical to the HIF-1 null mice, $CD34^+$ cell recruitment was virtually the same as that in wild-type mice.

Protein expression pattern in Matrigel-recruited cells. Results from the siRNA studies indicated that there was a complex pattern of protein-protein interactions in which the knockdown of TrxR led to lower levels of expression of Trx1 and HIF-1 in SPCs. This was also shown by Western blotting performed on lysed cells recovered from the Matrigel samples,

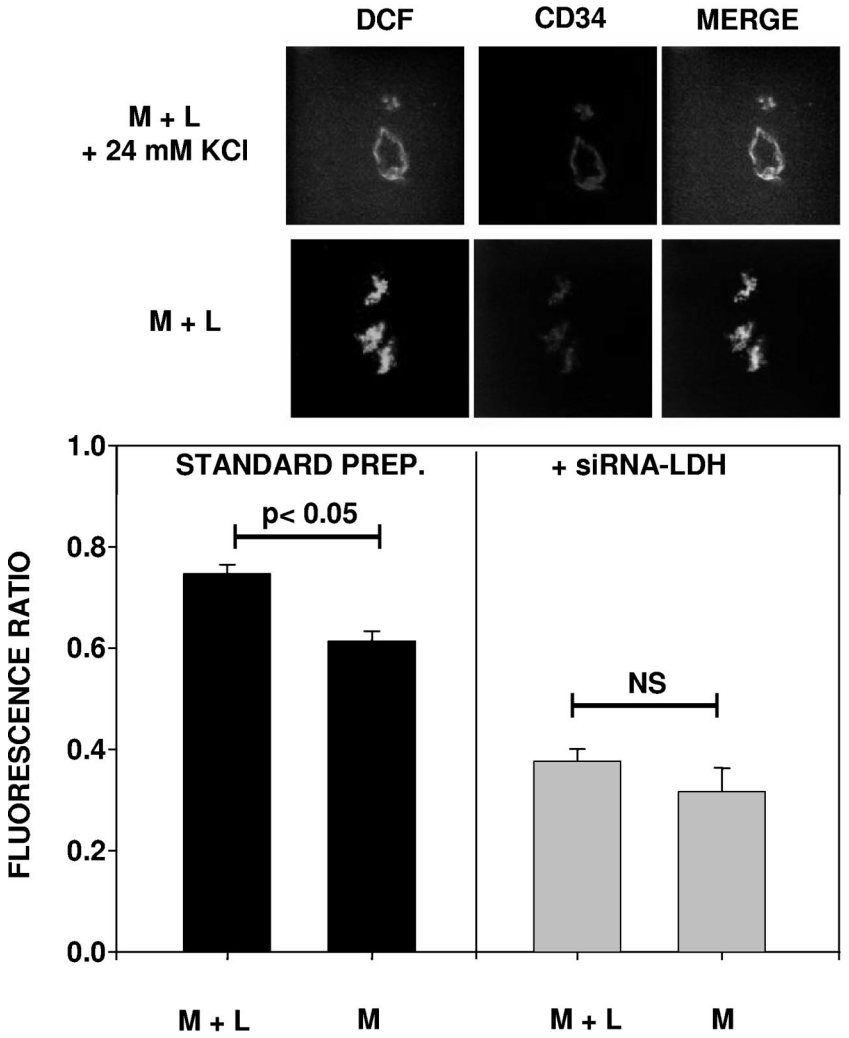

FIG. 5. DCF fluorescence in $CD34^+$ cell-lined channels within Matrigel. The top two rows of images show DCF fluorescence, as well as colocalization with the $CD34^+$ cells in a Matrigel-lactide sample (M + L) with and without the topical addition of 24 mM KCl to cause cell depolarization. The bar graphs at the bottom show the ratios of DCF fluorescence (without versus with KCl) from different Matrigel samples (n = 3 different mice for each calculation). Where indicated, Matrigel samples were supplemented with siRNA specific to LDH (+siRNA-LDH). The fluorescence in the standard-preparation (standard prep.) Matrigel-lactide samples and Matrigel samples (M) was significantly greater than that in the siRNA samples.

and there were smaller amounts of VEGF and SDF-1 in the cells deficient in TrxR (Fig. 7 and representative blots shown in Fig. 8 and 9). Ex vivo studies with endothelial cells and some tumor cells have shown the existence of an autocrine feedback loop involving HIF-1, VEGF, and ERK 1/2, so we evaluated the fractions of phosphorylated MAPKs in the Matrigel cell pellets (11, 48). As shown in Fig. 7, cells from lactate-supplemented Matrigel samples exhibited significantly higher proportions of phosphorylated ERK, JNK, and p38 and higher levels of expression of Trx1, TrxR, HIF-1, VEGF, and SDF-1 than cells from unsupplemented Matrigel samples.

We hypothesized that lactate metabolism causes oxidative stress and found that lactate effects on various proteins were inhibited in Matrigel that included LDH-specific siRNA, apocynin, DTE, or NAC (Fig. 7). Trx1, as well as ROS, can stimulate MAPK phosphorylation, and in turn, ERK 1/2 can stimulate Trx1 synthesis (2, 37). Matrigel containing U0126, a specific ERK 1/2 inhibitor, had significantly fewer $CD34^+$ cells than Matrigel without the inhibitor (Table 1) and a degree and pattern of protein synthesis inhibition similar to those seen with the other inhibitory agents, except that there was no reduction in the fraction of phosphorylated p38 MAPK. If lactate-supplemented Matrigel samples included siRNA specific to TrxR (but not nonsilencing control siRNA), the increases seen in MAPK phosphorylation and the various protein levels in lactate-supplemented Matrigel samples were abolished and the numbers of $CD34^+$ cells in Matrigel were reduced (Table 4; Fig. 7). The same pattern of effects was also observed in samples containing siRNA targeting HIF-1 and in samples from the conditionally HIF-1 null mice. Finally, consistent with the presence of an autocrine loop, antibodies to VEGF and SDF-1 also inhibited $CD34^+$ cell recruitment and the levels of the various proteins in the cells (Table 1; Fig. 7).

TABLE 4. Cell counts in Matrigel and flow cytometry-assessed contents of HIF-1 and Trx1 in cells[a]

Inhibitor	Sample type[b]	No. of $CD34^+$ cells (10^6)	Amt in $CD34^+$ cells of:		No. of $CD34^-$ $CD45^+$ cells (10^6)	Amt in $CD34^-$ $CD45^+$ cells of:	
			HIF-1	Trx1[e]		HIF-1	Trx1[e]
None (control)	M+L	4.21 ± 0.18	372.1 ± 8.8	388.7 ± 5.2	0.62 ± 0.02	23.5 ± 0.6	13.8 ± 0.2
	M	1.37 ± 0.08[c]	133.1 ± 1.2[c]	122.5 ± 0.5[c]	0.15 ± 0.01[c]	21.1 ± 0.7	13.1 ± 0.2
Control siRNA	M+L	3.82 ± 0.18	389.8 ± 4.6	365.2 ± 4.7	0.51 ± 0.01	24.1 ± 0.4	13.7 ± 0.1
	M	1.26 ± 0.12[c,d]	131.3 ± 0.8[c]	122.2 ± 2.1[c]	0.15 ± 0.01[c]	22.2 ± 0.9	13.1 ± 0.3
TrxR siRNA	M+L	1.23 ± 0.06[c]	203.2 ± 4.0[c]	135.2 ± 1.7[c]	0.015 ± 0.001	24.2 ± 0.1	12.1 ± 0.1
	M	0.65 ± 0.04[c,d]	97.3 ± 0.6[c,d]	77.9 ± 0.36[c,d]	0.003 ± 0.001[c,d]	23.2 ± 0.2	12.1 ± 0.1
HIF-1 siRNA	M+L	1.49 ± 0.04[c]	27.7 ± 0.7[c]		0.03 ± 0.01[c]	2.20 ± 0.17[c]	
	M	0.93 ± 0.07[c,d]	11.2 ± 0.2[c,d]		0.008 ± 0.001[c,d]	1.23 ± 0.03[c,d]	

[a] Values are means ± SE ($n = 3$) for each group. Levels of HIF-1 and Trx1 are expressed as relative fluorescence units.
[b] M, unsupplemented Matrigel; M+L, Matrigel supplemented with lactide.
[c] $P < 0.05$ versus value for control (M+L).
[d] $P < 0.05$ versus value for control (M).
[e] Trx1 in cells incubated with siRNA targeting HIF-1 was not evaluated by flow cytometry, but it was assessed by Western blotting (Fig. 7 and Table 5).

SPC cell cycle. The mitotic activity of $CD34^+$ cells in Matrigel was evaluated by determining the proportions of cells in the S or G_2/M phase of the cell cycle. The DNA content (propidium iodide uptake) was assessed by flow cytometry, and the cell cycle was analyzed using computer software. In unsupplemented Matrigel from control mice, 3.2% ± 0.1% ($n = 5$) of $CD34^+$ cells were in the S, G_2, or M phase, whereas the proportion in Matrigel-lactide samples was 15.5% ± 0.3% ($n = 5$; $P < 0.05$ versus the value for unsupplemented Matrigel). If the Matrigel contained siRNA targeting TrxR, 3.3% ± 0.3% ($n = 3$; NS versus the control value) of $CD34^+$ cells in the Matrigel-only samples were in the S, G_2, or M phase and

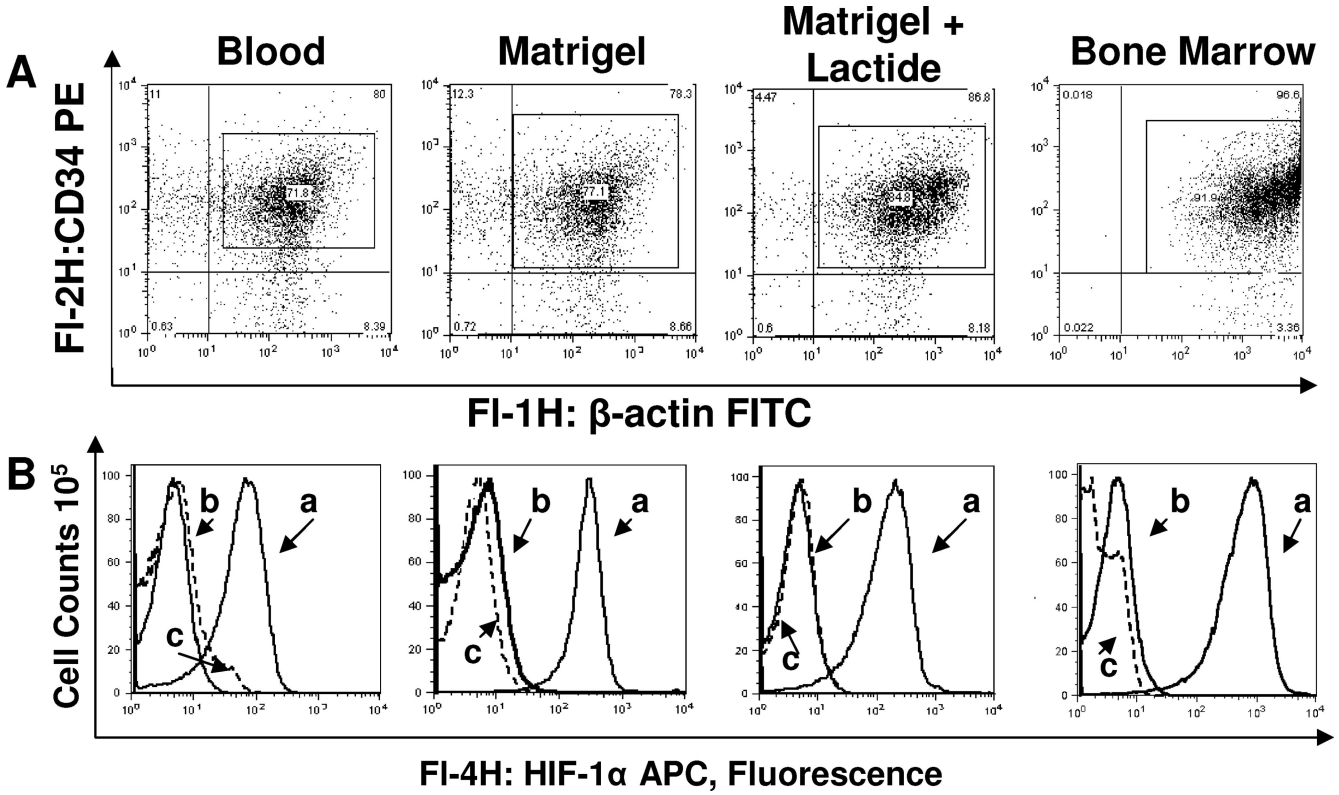

FIG. 6. Intracellular HIF-1 and β-actin in permeabilized $CD34^+$ cells assessed by flow cytometry. (A) Shown are representative dot plots for cells stained for β-actin. Among samples in each group (blood, Matrigel with and without lactide, and bone marrow), there were no significant differences in the magnitude of β-actin detected, thus demonstrating comparable degrees of permeabilization in all samples. (B) Cells were probed for HIF-1, and histograms were generated. Representative examples are shown. Curves labeled a are for cells from normal wild-type mice, curves labeled b are for $CD34^+$ cells from mice with conditionally HIF-1 null myeloid cells, and curves labeled *c* are for wild-type cells stained with nonspecific immunoglobulin G conjugated to APC.

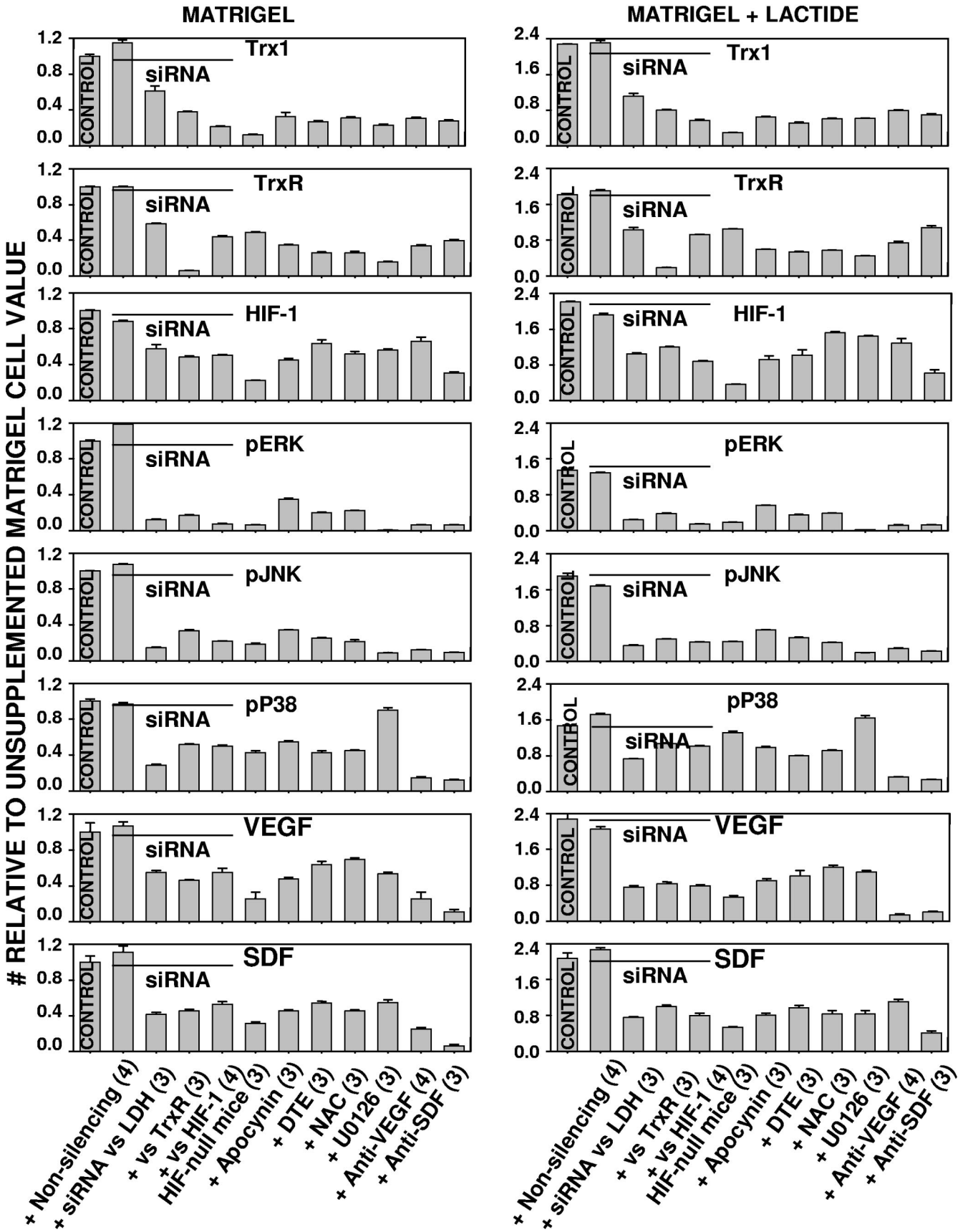
MATRIGEL
MATRIGEL + LACTIDE
RELATIVE TO UNSUPPLEMENTED MATRIGEL CELL VALUE
Trx1
TrxR
HIF-1
pERK
pJNK
pP38
VEGF
SDF
CONTROL
siRNA
+ Non-silencing (4)
+ siRNA vs LDH (3)
+ vs TrxR (3)
+ vs HIF-1 (4)
HIF-null mice (3)
+ Apocynin (3)
+ DTE (3)
+ NAC (3)
+ U0126 (3)
+ Anti-VEGF (4)
+ Anti-SDF (3)

TABLE 5. Selected enzymes in lysed cell pellets obtained from digested Matrigel plugs[a]

Inhibitor or mouse strain (no. of samples)	Sample type	% of total MAPK present as phospho-MAPK			Level of:				
		ERK 1/2	JNK	p38	Trx1	TrxR	HIF-1α	VEGF	SDF-1
No inhibitor (control; 4)	M+L	38.3 ± 0.43	35.3 ± 0.55	12.2 ± 0.09	2.24 ± 0.01	2.53 ± 0.01	2.69 ± 0.01	2.87 ± 0.12	2.56 ± 0.15
	M	28.2 ± 0.18	18.1 ± 0.03	8.3 ± 0.21	0.98 ± 0.02	1.40 ± 0.01	1.22 ± 0.01	1.22 ± 0.13	1.23 ± 0.09
Apocynin (3)	M+L	15.8 ± 0.25	12.9 ± 0.07	8.2 ± 0.15	0.63 ± 0.01	0.83 ± 0.01	1.12 ± 0.07	1.09 ± 0.06	0.99 ± 0.06
	M	9.80 ± 0.42	6.23 ± 0.09	4.50 ± 0.09	0.30 ± 0.03	0.48 ± 0.01	0.55 ± 0.02	0.58 ± 0.18	0.56 ± 0.02
DTE (3)	M+L	10.0 ± 0.21	9.6 ± 0.03	6.6 ± 0.10	0.50 ± 0.02	0.74 ± 0.02	1.81 ± 0.02	1.23 ± 0.15	1.20 ± 0.06
	M	5.6 ± 0.05	4.6 ± 0.12	3.53 ± 0.18	0.26 ± 0.01	0.36 ± 0.01	0.64 ± 0.01	0.77 ± 0.05	0.67 ± 0.02
NAC (3)	M+L	10.9 ± 0.18	8.8 ± 0.03	7.6 ± 0.11	0.60 ± 0.01	0.80 ± 0.01	1.85 ± 0.03	1.23 ± 0.15	1.20 ± 0.06
	M	6.2 ± 0.09	3.9 ± 0.41	3.73 ± 0.07	0.31 ± 0.01	0.36 ± 0.01	0.64 ± 0.03	0.77 ± 0.05	0.67 ± 0.02
U0126 (3)	M+L	0.06 ± 0.01	3.53 ± 0.07	13.6 ± 0.50†	0.60 ± 0.01	0.62 ± 0.02	1.75 ± 0.03	1.33 ± 0.03	1.36 ± 0.07
	M	0.23 ± 0.03	1.62 ± 0.04	7.10 ± 0.17†	0.22 ± 0.01	0.22 ± 0.01	0.68 ± 0.02	0.65 ± 0.03	0.68 ± 0.03
Control siRNA (6)	M+L	36.4 ± 0.26	30.5 ± 0.44	14.3 ± 0.15	2.45 ± 0.03	2.66 ± 0.03	2.34 ± 0.04	2.50 ± 0.06	2.80 ± 0.06
	M	24.1 ± 0.11	19.5 ± 0.15	8.03 ± 0.12	1.28 ± 0.02	1.50 ± 0.02	1.07 ± 0.02	1.30 ± 0.06	1.37 ± 0.06
LDH siRNA (3)	M+L	7.0 ± 0.07	6.5 ± 0.21	6.1 ± 0.09	1.1 ± 0.06	1.44 ± 0.09	1.27 ± 0.03	2.50 ± 0.06	2.80 ± 0.06
	M	3.5 ± 0.18	2.7 ± 0.12	2.4 ± 0.12	0.6 ± 0.06	0.82 ± 0.01	0.71 ± 0.06	1.30 ± 0.06	1.37 ± 0.06
TrxR siRNA (3)	M+L	10.8 ± 0.12	9.13 ± 0.07	8.90 ± 0.15	0.78 ± 0.02	0.26 ± 0.01	1.46 ± 0.01	1.02 ± 0.04	1.23 ± 0.03
	M	4.80 ± 0.26	6.03 ± 0.28	4.30 ± 0.06	0.37 ± 0.01	0.08 ± 0.01	0.59 ± 0.01	0.56 ± 0.01	0.56 ± 0.02
HIF-1α siRNA (4)	M+L	4.1 ± 0.10	7.93 ± 0.03	8.40 ± 0.12	0.55 ± 0.03	1.29 ± 0.01	1.07 ± 0.01	0.95 ± 0.06	0.99 ± 0.06
	M	2.03 ± 0.13	3.93 ± 0.09	4.13 ± 0.09	0.21 ± 0.01	0.61 ± 0.02	0.61 ± 0.01	0.67 ± 0.09	0.65 ± 0.04
HIF-1α null mice (3)	M+L	5.10 ± 0.12	7.95 ± 0.13	10.87 ± 0.35	0.28 ± 0.01	1.46 ± 0.01	0.44 ± 0.01	0.64 ± 0.05	0.65 ± 0.02
	M	1.87 ± 0.05	3.37 ± 0.15	3.53 ± 0.18	0.12 ± 0.01	0.68 ± 0.01	0.27 ± 0.01	0.31 ± 0.09	0.38 ± 0.02
Anti-VEGF (4)	M+L	3.5 ± 0.04	5.23 ± 0.28	2.67 ± 0.09	0.77 ± 0.02	1.03 ± 0.04	1.57 ± 0.12	0.16 ± 0.03	0.50 ± 0.06
	M	1.76 ± 0.09	2.20 ± 0.06	1.20 ± 0.12	0.30 ± 0.01	0.47 ± 0.02	0.80 ± 0.05	0.13 ± 0.03	0.31 ± 0.02
Anti-SDF-1 (3)	M+L	3.77 ± 0.09	4.23 ± 0.09	2.23 ± 0.09	0.68 ± 0.02	1.51 ± 0.06	0.75 ± 0.09	0.24 ± 0.02	0.12 ± 0.02
	M	1.87 ± 0.09	1.70 ± 0.06	1.04 ± 0.04	0.27 ± 0.01	0.55 ± 0.02	0.37 ± 0.01	0.12 ± 0.01	0.08 ± 0.01

[a] Comparisons were made between control Matrigel plugs containing no inhibitor and corresponding plugs containing each inhibitor shown and between Matrigel-lactide (M+L) and unsupplemented Matrigel (M) samples containing the same inhibitors. Phosphorylated MAPKs (phospho-MAPKs) were assessed as the percentages of phosphorylated ERK 1/2, JNK, and p38 among the total amounts of these kinases in the cell pellets. Band densities were evaluated relative to band densities for the total amount of the appropriate MAPK found on the same Western blots. In each group (control samples and samples containing inhibitors), the fractions of phosphorylated enzymes in cells from Matrigel-lactide samples were significantly different from those in cells from unsupplemented Matrigel samples. The fractions of phosphorylated enzymes in control Matrigel-lactide samples were significantly greater than those in all other samples except Matrigel-lactide samples containing control siRNA and the samples corresponding to values labeled with † in the p38 column. Similarly, the fractions of phosphorylated enzymes in control Matrigel samples were significantly greater than those in all other Matrigel samples except Matrigel samples containing control siRNA. The contents of proteins (Trx1, TrxR, HIF-1, VEGF, and SDF-1) in the cells are expressed as the ratios of the band densities on Western blots to the band densities for β-actin on the same blots. All values are means ± SE.

the proportion in Matrigel-lactide samples was 8.6% ± 0.1% ($n = 3$; $P < 0.05$ versus the control value). If the Matrigel contained siRNA specific to HIF-1, 2.0% ± 0.1% ($n = 4$; NS versus the control value) of $CD34^+$ cells in the Matrigel-only samples were in the S, G_2, or M phase and the proportion in Matrigel-lactide samples was 4.9% ± 0.1% ($n = 4$; $P < 0.05$ versus the control value). Conditionally HIF-1 null mice exhibited a pattern similar to that seen with the siRNA targeting

FIG. 7. Protein expression patterns in cells found in Matrigel. Cell lysates were subjected to Western blotting as outlined in Materials and Methods. All values were normalized to the protein concentration found in cells isolated from unsupplemented Matrigel. The actual values for each sample can be found in Table 5. Agents were added to Matrigel or Matrigel-lactide as indicated on the abscissas. Wild-type mice were used in all cases, except where the bars are indicated to represent results for mice with conditionally HIF-1 null myeloid cells. Agents included in the Matrigel samples were nonsilencing control siRNA; siRNA directed against LDH, TrxR, or HIF-1; apocynin; DTE; NAC; U0126; anti-VEGF antibody; or anti-SDF antibody. The contents of proteins (Trx1, TrxR, HIF-1, VEGF, and SDF) in cells were expressed as the ratios of the band densities on Western blots to the β-actin band densities on the same blots. In all cases, except those involving Matrigel containing nonsilencing control siRNA, values for cells isolated from Matrigel with inhibitors were lower than the values for cells isolated from Matrigel without inhibitors. In all cases, the protein contents of cells isolated from Matrigel-lactide were significantly greater than those of cells isolated from Matrigel that did not contain lactide. Phosphorylated enzymes were evaluated as ratios compared to the total amount of the enzymes in cells. The fractions in cells from Matrigel-lactide were significantly greater than those in cells from unsupplemented Matrigel. The fractions of phosphorylated enzymes in cells from samples with inhibitors were significantly reduced compared to those in the control cells, except for the fractions in cells containing nonsilencing control siRNA and the phosphorylated p38 content in cells from samples containing U0126. Numbers in parentheses are the numbers of samples in the indicated groups. pERK, pJNK, and pP38, phosphorylated ERK, JNK, and p38.

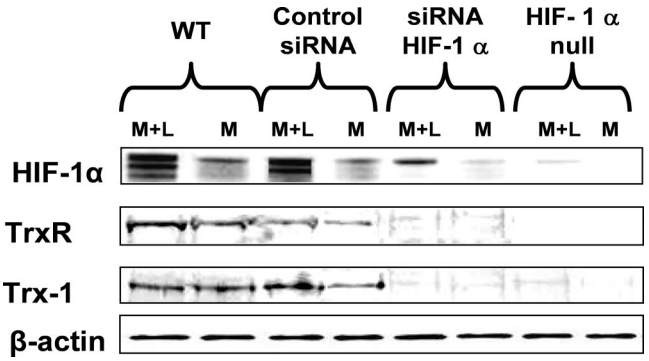

FIG. 8. Representative Western blot demonstrating the presence of HIF-1, TrxR, and Trx1, as well as β-actin, in cell lysates from Matrigel implanted into wild-type (WT) mice, Matrigel containing either nonsilencing control siRNA or siRNA specific to HIF-1 implanted into wild-type mice, and Matrigel implanted into mice with conditionally HIF-1 null myeloid cells. M, unsupplemented Matrigel samples; M+L, Matrigel-lactide samples.

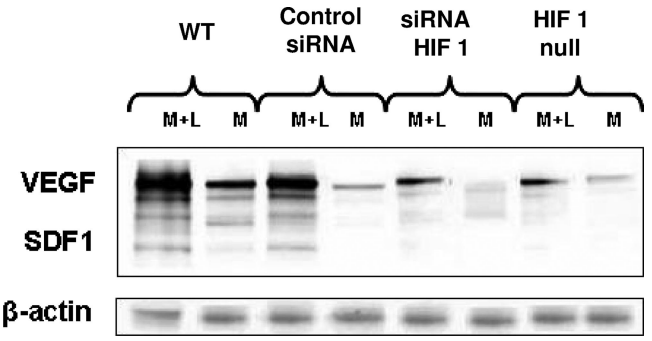

FIG. 9. Representative Western blot demonstrating the presence of VEGF and SDF-1, as well as β-actin, in cell lysates from Matrigel implanted into wild-type (WT) mice, Matrigel containing either nonsilencing control siRNA or siRNA specific to HIF-1 implanted into wild-type mice, and Matrigel implanted into mice with conditionally HIF-1 null myeloid cells. M, unsupplemented Matrigel samples; M+L, Matrigel-lactide samples.

HIF-1. In Matrigel samples from control mice that expressed HIF-1 but were otherwise genetically identical to the HIF-1 null mice, 3.9% ± 0.1% ($n = 4$) of $CD34^+$ cells were in the S, G_2, or M phase whereas the proportion in Matrigel-lactide samples was 15.1% ± 0.3% ($n = 4$; $P < 0.05$ versus the result for unsupplemented Matrigel). The proportions of S-, G_2-, or M-phase $CD34^+$ cells from HIF-1 null mice were as follows: 2.1% ± 0.1% ($n = 4$; $P < 0.05$ versus the control value) in unsupplemented Matrigel and 4.8% ± 0.2% ($n = 4$; $P < 0.05$ versus the control value) in Matrigel-lactide.

Blood and bone marrow responses. There appeared to be a systemic response to the Matrigel implants, because the numbers of $CD34^+$ cells in blood increased over time, although the total white-cell counts did not change. At the outset, the $CD34^+$ cell count was $0.4 \times 10^6 \pm 0.05 \times 10^6$/ml ($n = 10$); it increased to $1.0 \times 10^6 \pm 0.1 \times 10^6$/ml ($n = 4$; NS) at day 5 and to $1.5 \times 10^6 \pm 0.4 \times 10^6$/ml ($n = 5$; $P < 0.05$) at day 10. Because of this observation, we investigated the $CD34^+$ fractions and total cell counts in bone marrow samples. If mice were implanted with only unsupplemented Matrigel (different from the usual protocol of implanting two plugs, one containing lactide), after 1, 5, or 10 days the absolute cell counts and the proportions of $CD34^+$ cells in bone marrow samples were insignificantly different from those in samples from mice without implants, $4.2 \times 10^6 \pm 0.08 \times 10^6$/ml, with 13.4% ± 0.2% $CD34^+$ cells. Among mice implanted with lactide-containing Matrigel, the bone marrow cell counts were as follows ($n = 5$ for each group): on day 1, $6.4 \times 10^6 \pm 0.3 \times 10^6$/ml, with 28.1% ± 3.3% $CD34^+$; on day 5, $12.2 \times 10^6 \pm 3.5 \times 10^6$/ml, with 54.3% ± 3.4% $CD34^+$; and on day 10, $13.3 \times 10^6 \pm 2.3 \times 10^6$/ml, with 68.7 ± 4.0% $CD34^+$ (all values were significantly greater than values for mice implanted with unsupplemented Matrigel). The effect of lactide-containing Matrigel plugs on bone marrow cell counts was inhibited if Matrigel included oxamate, NAC, DTE, or U0126, LDH-, TrxR-, or HIF-1-specific siRNA, or antibodies against VEGF or SDF-1. With the inclusion of these inhibitors, the cell counts and the proportions of cells expressing CD34 were not different from those in samples from mice implanted with unsupplemented Matrigel (data not shown).

DISCUSSION

The Matrigel model allows a quantitative evaluation of in vivo SPC recruitment and growth responses. At 18 h after implantation, over 90% of the cells present in Matrigel expressed surface markers for SPCs and there were threefold more $CD34^+$ cells in Matrigel supplemented with the lactate polymer than in unsupplemented Matrigel. Dim expression of CD45 is typically used to exclude leukocytes while enumerating SPCs (7, 27). We were surprised by how few leukocytes were in samples harvested 18 h after implantation. There was no significant increase in the numbers of SPCs in Matrigel between days 5 and 10, suggesting that homing stimuli for SPCs are transient (Fig. 1). On day 10, there were actually fewer SPCs in Matrigel-lactide than there were on day 5. This finding may be due to differentiation and the loss of the CD34 marker or apoptosis due to the loss of trophic signals.

Whereas a very small fraction of $CD34^+$ cells in Matrigel expressed CD45 at 18 h postimplantation, the proportion of such cells in Matrigel harvested at 5 days increased significantly (Table 2). To assess whether SPCs may actually contribute to the leukocyte pool of cells, we removed Matrigel from mice at 18 h and cultured it ex vivo for 7 days. The marked elevation in cells coexpressing CD45 after this incubation (Table 2) indicates that some SPCs differentiate into myeloid cells. The pluripotency of SPCs is a matter of intense debate in the context of vasculogenesis. Because we observed erythrocytes in the Matrigel channels, we also assessed the expression of TER119 by $CD34^+$ cells. The results suggest that some recruited cells did form erythroid precursors (Table 2).

An intricate network of channels within Matrigel was shown to connect to the mouse vasculature based on analysis with fluorescent dextran or Nile red beads (Fig. 2). We conclude that this network was a manifestation of vasculogenesis because channels were lined with $CD34^+$ cells, many also expressed the EPC marker CD31, and many appeared to be undergoing proliferation, based on the expression of Ki67. The

presence of cell clumps versus linear channels in Matrigel incubated ex vivo (Fig. 2) is consistent with published findings that shear stress appears to be required for vascular channel formation (56, 59). The coexpression of some endothelial markers is influenced by shear stress (56, 59). The expression of vWF on endothelial cells is a dynamic process that is also influenced by growth factors and lactate (16, 20). At 18 h postimplantation, a higher percentage of $CD34^+$ cells from Matrigel-lactide samples than from unsupplemented Matrigel samples did express vWF (Table 3).

LDH can influence ROS production by providing NADH to Nox enzymes (19, 31), and this pathway appears to have been operating in SPCs based on DCF fluorescence in Matrigel (Fig. 5). The inhibitory effects of apocynin, oxamate, NAC, DTE, and siRNA specific to LDH on SPC recruitment and protein expression (Table 1; Fig. 7) indicate that ROS are a trophic stimulus of SPCs. The Trx system responds to oxidative stress by reducing ROS and also by promoting the expression and activity of HIF-1 (12, 26, 55). The pathway we propose for lactate enhancement of SPC recruitment to Matrigel is shown in Fig. 10. Oxamate and siRNA specific to LDH also exhibited adverse effects on $CD34^+$ cell recruitment and protein synthesis in unsupplemented Matrigel (Table 1; Fig. 7). We believe this effect is because unsupplemented Matrigel contains ~3 mM lactate.

Trx1 can bind to a number of transcription factors and signaling molecules (34). A role of the Trx system in SPCs was shown by the inhibitory actions of siRNA targeting TrxR. There were substantial elevations of Trx1 protein and TrxR in SPCs from lactate-supplemented versus unsupplemented Matrigel (Table 4; Fig. 7). The complexity of the mechanism responsible for this enhancement was shown by finding that siRNA specific to TrxR diminished the contents of Trx1 and HIF-1 in $CD34^+$ cells (Table 4). In this regard, finding no difference in Trx1 or HIF-1 levels in $CD45^+$ cells isolated from unsupplemented versus lactate-supplemented Matrigel offers circumstantial evidence that the robust SPC responses observed in this in vivo model were not related to metabolism by leukocytes following their influx into Matrigel.

When siRNA specific to TrxR or HIF-1 was added to the lactate-supplemented Matrigel, the number of $CD34^+$ cells present 18 h after implantation was reduced (Table 4). These results, along with findings for mice with conditionally HIF-1 null myeloid cells (Table 1), indicate that the influence lactate has on SPCs is mediated by HIF-1. Results for the conditionally HIF-1 null mice demonstrate several interesting points. There were significantly fewer $CD34^+$ cells in Matrigel harvested from conditionally HIF-1 null mice than in Matrigel harvested from wild-type mice 18 h after implantation (Table 1). Clearly, the presence of more $CD34^+$ cells in blood does not necessarily lead to more cell recruitment to Matrigel, as the conditionally HIF-1 null mice had eightfold more $CD34^+$ cells in their blood than the wild-type controls. Also, although the HIF-1 concentration was low, it was detectable in the cells isolated from Matrigel harvested from the HIF-1 null mice. This result may have occurred because not all SPCs express lysozyme (which is required to activate Cre and subsequently remove the HIF-1 locus in myeloid cells from these mice). There also may have been a small population of SPCs that expressed the same surface markers that we found (Table 3) but came from the walls of blood vessels near the Matrigel implants. These cells are not thought to be derived from bone marrow cells (41).

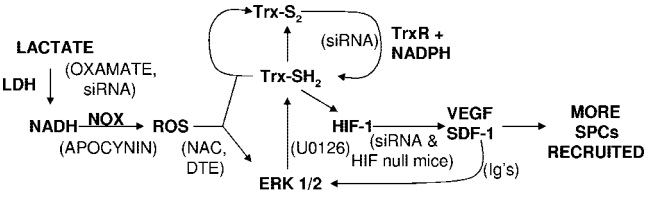

FIG. 10. Diagram showing the hypothesized sequence of effects triggered by lactate that stimulate SPC recruitment to Matrigel based on experimental findings. Items in parentheses are inhibitors used in this investigation to assess the roles of various agents in the pathway. Trx-S_2, oxidized thioredoxin; Trx-SH_2, reduced thioredoxin; Ig's, immunoglobulin antibodies to VEGF or SDF-1.

The results presented in Table 1 demonstrate that blocking the action of VEGF or SDF-1 with antibodies impaired SPC recruitment. VEGF and SDF-1 are regulated by HIF-1, and the inhibitory effects of antibodies against VEGF or SDF-1 present in the Matrigel were consistent with the findings reported in published literature on SPC homing (6, 24, 43). Contrary to expectations, however, cells harvested from Matrigel containing antibodies to growth factors exhibited reductions in the amounts of growth factor proteins, as well as Trx1, TrxR, and HIF-1, compared to the amounts in cells from Matrigel without antibodies (Fig. 7). The protein contents of the cell pellets were normalized to the amounts of β-actin present in the samples, so the diminished protein contents cannot be explained because there were fewer cells. These findings, as well as the finding of smaller fractions of phosphorylated MAPKs, demonstrate a complex interplay whereby abrogating effects of any component in the sequence outlined in Fig. 10 will inhibit the production of all other components.

Endothelial cells and macrophages increase VEGF synthesis when incubated in the presence of lactate (8, 30). The data from siRNA experiments and those with HIF-1 null mice indicate that the augmented synthesis of growth factors in lactate-supplemented Matrigel was due to HIF-1 (Fig. 7). Over 90% of the cells in Matrigel at 18 h postimplantation were SPCs, and lactate caused no elevation of Trx1 or HIF-1 in the few $CD45^+$ cells present. From these observations, we conclude that lactate caused SPCs themselves to generate the growth factors that hastened recruitment and cell differentiation, based on surface marker expression (Tables 2 and 3) and the proportion that had entered the cell cycle. It also appears that mediators enter the bloodstream and stimulate bone marrow SPCs, because mice injected with lactide-containing Matrigel had higher counts of circulating $CD34^+$ cells, higher bone marrow cell counts, and a greater proportion of bone marrow cells expressing CD34 than mice implanted with unsupplemented Matrigel.

In summary, multiple lines of evidence demonstrate that lactate influences SPC recruitment and differentiation in a pathway involving Trx1 and HIF-1. The repair of human skin after wounding is a lifelong process, so understanding the physiology has major clinical importance. Tumor growth also requires blood vessel development, and insight into how this occurs has important therapeutic implications. Our observa-

tions demonstrate that Trx1 and HIF-1 play major roles in SPC recruitment, growth, and differentiation. Lactate elevation is a ubiquitous characteristic of tumors and wounds. Hence, these findings offer important insights into the nature of vasculogenesis that may translate to direct clinical relevance.

ACKNOWLEDGMENTS

This work was supported by grants from the Office of Naval Research and from the NIH (DK080376 and GM081570).

REFERENCES

1. **Ali, M., F. Yasui, S. Matsugo, and T. Konishi.** 2000. The lactate-dependent enhancement of hydroxyl radical generation by the Fenton reaction. Free Radic. Res. **32:**429–438.
2. **Andoh, T., C. Chiueh, and P. Chock.** 2003. Cyclic GMP-dependent protein kinase regulates the expression of thioredoxin and thioredoxin peroxidase-1 during hormesis in response to oxidative stress-induced apoptosis. J. Biol. Chem. **278:**885–890.
3. **Arai, R., H. Masutani, J. Yodoi, V. Debbas, F. Laurindo, A. Stern, and H. Monteiro.** 2006. Nitric oxide induces thioredoxin-1 nuclear translocation: possible association with the p21Ras survival pathway. Biochem. Biophys. Res. Commun. **348:**1254–1260.
4. **Asahara, T., T. Murohara, A. Sullivan, M. Silver, R. van der Zee, T. Li, B. Witzenbichler, G. Schatteman, and J. M. Isner.** 1997. Isolation of putative progenitor endothelial cells for angiogenesis. Science **275:**964–967.
5. **Balasubramaniam, V., C. F. Mervis, A. M. Maxey, N. E. Markham, and S. H. Abman.** 2007. Hyperoxia reduces bone marrow, circulating, and lung endothelial progenitor cells in the developing lung: implications for the pathogenesis of bronchopulmonary dysplasia. Am. J. Physiol. Lung Cell. Mol. Physiol. **292:**L1073–L1084.
6. **Ceradini, D. J., A. R. Kulkarni, M. J. Callaghan, O. M. Tepper, N. Bastidas, M. E. Kleinman, J. M. Capla, R. D. Galiano, J. P. Levine, and G. C. Gurtner.** 2004. Progenitor cell trafficking is regulated by hypoxic gradients through HIF-1 induction of SDF-1. Nat. Med. **10:**858–864.
7. **Chin-Yee, I., M. Keeney, L. Anderson, R. Nayar, and D. Sutherland.** 1997. Current status of $CD34^+$ cell analysis by flow cytometry: the ISHAGE guidelines. Clin. Immunol. Newsl. **17:**21–29.
8. **Constant, J. S., J. J. Feng, D. D. Zabel, H. Yuan, D. Y. Suh, H. Scheuenstuhl, T. K. Hunt, and M. Z. Hussain.** 2000. Lactate elicits vascular endothelial growth factor from macrophages: a possible alternative to hypoxia. Wound Repair Regen. **8:**353–360.
9. **Cramer, T., Y. Yamanishi, B. Clausen, I. Forster, R. Pawlinski, M. Mackman, V. Haase, R. Jaenisch, M. Corr, V. Nizet, G. Firestein, H. Gerber, N. Ferrara, and R. Johnson.** 2003. HIF-1a is essential for myeloid cell-mediated inflammation. Cell **112:**645–657.
10. **Crowther, M., N. Brown, E. Bishop, and C. Lewis.** 2001. Microenvironmental influence on macrophage regulation of angiogenesis in wounds and malignant tumors. J. Leukoc. Biol. **70:**478–490.
11. **Das, B., H. Yeger, R. Tsuchida, R. Torkin, M. Gee, P. Thorner, M. Shibuya, D. Malkin, and S. Baruchel.** 2005. A hypoxia-driven vascular endothelial growth factor/Flt1 autocrine loop interacts with hypoxia-inducible factor-1α through mitogen-activated protein kinase/extracellular signal-regulated kinase 1/2 pathway in neuroblastoma. Cancer Res. **65:**7267–7275.
12. **Ema, M., K. Hirota, J. Mimura, H. Abe, J. Yodoi, K. Sogawa, L. Poellinger, and Y. Fujii-Kuriyama.** 1999. Molecular mechanisms of transcription activation by HLF and HIF1α in response to hypoxia: their stabilization and redox signal-induced interaction with CBP/p300. EMBO J. **18:**1905–1914.
13. **Ghani, Q., S. Wagner, and M. Hussain.** 2003. Role of ADP ribosylation in wound repair: the contributions of Thomas K. Hunt. Wound Repair Regen. **11:**439–444.
14. **Gladden, L.** 2004. Lactate metabolism: a new paradigm for the third millennium. J. Physiol. **558:**5–30.
15. **Goldstein, L. J., K. A. Gallagher, S. M. Bauer, R. J. Bauer, V. Baireddy, Z. J. Liu, D. G. Buerk, S. R. Thom, and O. C. Velazquez.** 2006. Endothelial progenitor cell release into circulation is triggered by hyperoxia-induced increases in bone marrow nitric oxide. Stem Cells **24:**2309–2318.
16. **Gottfried, E., K. Kreutz, S. Haffner, E. Holler, M. Iacobelli, R. Andreesen, and G. Eissner.** 2007. Differentiation of human tumour-associated dendritic cells into endothelial-like cells: an alternative pathway of tumour angiogenesis. Scand. J. Immunol. **65:**329–335.
17. **Gratama, J. W., A. Orfao, D. Barnett, B. Brando, A. Huber, G. Janossy, H. E. Johnson, M. Keeney, G. E. Marti, F. Preijers, G. Rothe, S. Serke, D. R. Sutherland, C. E. Vander Schoot, G. Schmitz, and S. Papa.** 1998. Flow cytometric enumeration of $Cd34^+$ hematopoietic stem and progenitor cells. Cytometry **34:**128–142.
18. **Grunewald, M., I. Avraham, Y. Dor, E. Bachar-Lustig, A. Itin, S. Jung, S. Chimenti, L. Landsman, R. Abramovitch, and E. Keshet.** 2006. VEGF-induced adult neovascularization: recruitment, retention, and role of accessory cells. Cell **124:**175–189.
19. **Gupte, S., T. Rupawalla, H. Mohazzab, and M. Wolin.** 1999. Regulation of NO-elicited pulmonary artery relaxation and guanylate cyclase activation by HADH oxidase and SOD. Am. J. Physiol. Heart Circ. Physiol. **276:**H1535–H1542.
20. **Hannah, M., P. Skehel, M. Erent, L. Knipe, D. Ogden, and T. Carter.** 2005. Differential kinetics of cell surface loss of von Willebrand factor and its propolypeptide after secretion from Weibel-Palade bodies in living human endothelial cells. J. Biol. Chem. **280:**22827–22830.
21. **Hattori, I., Y. Yakagi, K. Nozaki, N. Kondo, J. Bai, H. Nakamura, N. Hashimoto, and J. Yodoi.** 2002. Hypoxia-ischemia induces thioredoxin expression and nitrotyrosine formation in new-born rat brain. Redox Rep. **7:**256–259.
22. **Hattori, K., S. Dias, B. Heissig, N. R. Hackett, D. Lycen, M. Tateno, D. J. Hicklin, Z. Zhu, L. Witte, R. G. Crystal, M. A. Moore, and S. Rafii.** 2001. Vascular endothelial growth factor and angiopoietin-1 stimulate postnatal hematopoiesis by recruitment of vasculogenic and hematopoietic stem cells. J. Exp. Med. **193:**1005–1014.
23. **Hunt, T., R. Aslam, S. Beckert, S. Wagner, Q. Ghani, M. Hussain, S. Roy, and C. Sen.** 2007. Aerobically derived lactate stimulates revascularization and tissue repair via redox mechanisms. Antioxid. Redox Signal. **9:**1115–1124.
24. **Jiang, M., B. Wang, C. Wang, B. He, H. Fan, T. Guo, Q. Shao, L. Gao, and Y. Liu.** 2006. Inhibition of hypoxia-inducible factor-1 and endothelial progenitor cell differentiation by adenoviral transfer of small interfering RNA in vitro. J. Vasc. Res. **43:**511–521.
25. **Jin, D. K., K. Shido, H. G. Kopp, I. Petit, S. V. Shmelkov, L. M. Young, A. T. Hooper, H. Amano, S. T. Avecilla, B. Heissig, K. Hattori, F. Zhang, D. J. Hicklin, Y. Wu, Z. Zhu, A. Dunn, H. Salari, Z. Werb, N. R. Hackett, R. G. Crystal, D. Lyden, and S. Rafii.** 2006. Cytokine-mediated deployment of SDF-1 induces revascularization through recruitment of $CXCR4^+$ hemangiocytes. Nat. Med. **12:**557–567.
26. **Kaga, S., L. Zhan, M. Matusmoto, and N. Maulik.** 2005. Resveratrol enhances neovascularization in the infarcted rat myocardium through the induction of thioredoxin-1, heme oxygenase-1 and vascular endothelial growth factor. J. Mol. Cell. Cardiol. **38:**813–822.
27. **Keeney, M., I. Chin-Yee, K. Weir, J. Popma, R. Nayar, and D. Sutherland.** 1998. Single platform flow cytometric absolute $CD34^+$ cell counts based on the ISHAGE guidelines. Cytometry **34:**61–70.
28. **Kina, T., K. Ikuta, E. Takayama, K. Wada, A. Majumdar, I. Weissman, and Y. Katsura.** 2000. The monoclonal antibody TER-119 recognizes a molecule associated with glycophorin A and specifically marks the late stages of murine erythroid lineage. Br. J. Haematol. **109:**280–287.
29. **Kleinman, H. K., M. L. McGarvey, L. A. Liotta, P. G. Robey, K. Tryggvason, and G. R. Martin.** 1982. Isolation and characterization of type IV procollagen, laminin, and heparin sulfate proteoglycan from the EHS sarcoma. Biochemistry **21:**6188–6193.
30. **Kumar, V. B. S., R. I. Viji, M. S. Kiran, and P. R. Sudhakaran.** 2007. Endothelial cell response to lactate: implication of PAR modification of VEGF. J. Cell. Physiol. **211:**477–485.
31. **Lee, Y., I. Kang, R. Bunger, and Y. Kang.** 2004. Enhanced survival effect of pyruvate correlates MAPK and NFκB activation in hydrogen peroxide-treated human endothelial cells. J. Appl. Physiol. **96:**793–801.
32. **Lu, H., R. Forbes, and A. Verma.** 2002. Hypoxia-inducible factor-1 activation by aerobic glycolysis implicates the Warburg effect in carcinogenesis. J. Biol. Chem. **277:**23111–23115.
33. **Massberg, S., I. Konrad, K. Schurzinger, M. Lorenz, S. Schneider, D. Zohlnhoefer, K. Hoppe, M. Schiemann, E. Kennerknecht, S. Sauer, C. Schulz, S. Kerstan, M. Rudelius, S. Seidl, F. Sorge, H. Langer, M. Peluso, P. Goyal, D. Vestweber, N. R. Emambokus, D. H. Busch, J. Frampton, and M. Gawaz.** 2006. Platelets secrete stromal cell-derived factor 1α and recruit bone marrow-derived progenitor cells to arterial thrombi in vivo. J. Exp. Med. **203:**1221–1233.
34. **Maulik, N., and D. Das.** 16 January 2008. Emerging potential of thioredoxin and thioredoxin interacting proteins in various disease conditions. Biochim. Biophys. Acta. [Epub ahead of print.] doi:10.1016/j.bbagen.2007.12.008.
35. **McClendon, S., N. Zhadin, and R. Callender.** 2005. The approach to the Michaelis complex in lactate dehydrogenase: the substrate binding pathway. Biophys. J. **89:**2024–2032.
36. **Nakamura, H., M. Matsuda, K. Furuke, Y. Kitaoka, S. Iwata, K. Toda, T. Inamoto, Y. Yamaoka, K. Ozawa, and J. Yodoi.** 1994. Adult T cell leukemia-derived factor/human thioredoxin protects endothelial F-2 cell injury caused by activated neutrophils or hydrogen peroxide. Immunol. Lett. **41:**75–80.
37. **Pekkari, K., M. Goodarzi, A. Scheynius, A. Holmgren, and J. Avila-Carino.** 2005. Truncated thioredoxin (Trx80) induces differentiation of human $CD14^+$ monocytes into a novel cell type (TAMs) via activation of MAP kinases p38, ERK, and JNK. Blood **105:**1598–1605.
38. **Poli, G., G. Leonarduzzi, F. Biasi, and E. Chiarpotto.** 2004. Oxidative stress and cell signalling. Curr. Med. Chem. **11:**1163–1182.
39. **Rajantie, I., M. Ilmonen, A. Alminaite, U. Ozerdem, K. Alitalo, and P. Salven.** 2004. Adult bone marrow-derived cells recruited during angiogenesis comprise precursors for periendothelial vascular mural cells. Blood **104:**2084–2086.

40. **Sachi, Y., K. Hirota, H. Masutani, K. Toda, T. Okamoto, M. Takigawa, and J. Yodoi.** 1995. Induction of ADF/TRX by oxidative stress in keratinocytes and lymphoid cells. Immunol. Lett. **44:**189–193.
41. **Sainz, J., A. Zen, G. Caligiuri, C. Demerens, D. Urbain, M. Lemitre, and A. Lafont.** 2006. Isolation of "side population" progenitor cells from healthy arteries of adult mice. Arterioscler. Thromb. Vasc. Biol. **26:**281–286.
42. **Salceda, S., and J. Caro.** 1997. Hypoxia-inducible factor 1 alpha protein is rapidly degraded by the ubiquitin-proteasome system under normoxic conditions: its stabilization by hypoxia depends upon redox-induced changes. J. Biol. Chem. **272:**22642–22647.
43. **Semenza, G.** 2000. Surviving ischemia: adaptive responses mediated by hypoxia-inducible factor 1. J. Clin. Investig. **106:**809–812.
44. **Semenza, G. L.** 2001. HIF-1 and mechanisms of hypoxia sensing. Curr. Opin. Cell Biol. **13:**167–171.
45. **Sen, C., S. Khanna, B. Babior, T. Hunt, E. Ellison, and S. Roy.** 2002. Oxidant-induced vascular endothelial growth factor expression in human keratinocytes and cutaneous wound healing. J. Biol. Chem. **277:**33284–33290.
46. **Sivan-Loukianova, E., O. A. Awad, V. Stepanovic, J. Bickenbach, and G. C. Schatteman.** 2003. $CD34^+$ blood cells accelerate vascularization and healing of diabetic mouse skin wounds. J. Vasc. Res. **40:**368–377.
47. **Springer, M., T. Ip, and H. Blau.** 2000. Angiogenesis monitored by perfusion with a space-filling microbead suspension. Mol. Ther. **1:**82–87.
48. **Tang, N., L. Wang, J. Esko, F. Giordano, Y. Huang, H.-P. Gerber, N. Ferrara, and R. Johnson.** 2004. Loss of HIF-1α in endothelial cells disrupts a hypoxia-driven VEGF autocrine loop necessary for tumorigenesis. Cancer Cell **6:**485–495.
49. **Thom, S. R., V. M. Bhopale, O. C. Velazquez, L. J. Goldstein, L. H. Thom, and D. G. Buerk.** 2006. Stem cell mobilization by hyperbaric oxygen. Am. J. Physiol. Heart Circ. Physiol. **290:**H1378–H1386.
50. **To, L. B., D. N. Haylock, P. J. Simmons, and C. A. Juttner.** 1997. The biology and clinical uses of blood stem cells. Blood **89:**2233–2258.
51. **Trabold, O., S. Wagner, C. Wicke, H. Scheuenstuhl, M. Z. Hussain, N. Rosen, A. Seremetiev, H. D. Becker, and T. K. Hunt.** 2003. Lactate and oxygen constitute a fundamental regulatory mechanism in wound healing. Wound Repair Regen. **11:**504–509.
52. **Tung, J. W., D. R. Parks, W. A. Moore, L. A. Herzenberg, and L. A. Herzenberg.** 2004. New approaches to fluorescence compensation and visualization of FACS data. Clin. Immunol. **110:**277–283.
53. **Walenta, S., A. Salameh, H. Lyng, J. Evensen, M. Mitze, E. Rofstad, and W. Mueller-Klieser.** 1997. Correlation of high lactate level in head and neck tumors with incidence of metastasis. Am. J. Pathol. **150:**409–415.
54. **Watson, W., J. Heilman, L. Hughes, and J. Spielberger.** 2008. Thioredoxin reductase-1 knock down does not result in thioredoxin-1 oxidation. Biochem. Biophys. Res. Commun. **368:**832–836.
55. **Welsh, S., W. Bellamy, M. Briehl, and G. Powis.** 2002. The redox protein thioredoxin-1 (Trx-1) increases hypoxia-inducible factor-1α protein expression: Trx-1 overexpression results in increased vascular endothelial growth factor production and enhanced tumor angiogenesis. Cancer Res. **62:**5089–5095.
56. **Yamamoto, K., T. Takahashi, T. Asahara, N. Ohura, T. Sokabe, A. Kamiya, and J. Ando.** 2003. Proliferation, differentiation, and tube formation by endothelial progenitor cells in response to shear stress. J. Appl. Physiol. **95:**2081–2088.
57. **Ye, M., H. Iwasaki, C. Laiosa, M. Stadtfeld, H. Xie, S. Heck, B. Clausen, K. Akashi, and T. Graf.** 2003. Hematopoietic stem cells expressing the myeloid lysozyme gene retain long-term, multilineage repopulation potential. Immunity **19:**689–699.
58. **Zeigelhoeffer, T., B. Fernandez, S. Kostin, M. Heil, R. Voswinckel, A. Helisch, and W. Schaper.** 2004. Bone marrow-derived cells do not incorporate into the adult growing vasculature. Circ. Res. **94:**230–238.
59. **Zeng, L., Q. Xiao, A. Margariti, Z. Zhang, A. Zampetaki, S. Patel, M. Capogrossi, Y. Hu, and Q. Xu.** 2006. HDAC3 is crucial in shear- and VEGF-induced stem cell differentiation toward endothelial cells. J. Cell Biol. **174:**1059–1069.
60. **Zieker, D., R. Schäfer, J. Glatzle, K. Nieselt, S. Coerper, H. Northoff, A. Königsrainer, T. K. Hunt, and S. Beckert.** 2008. Lactate modulates gene expression in human mesenchymal stem cells. Langenbeck's Arch. Surg. **393:**297–301.